LUND UNIVERSITY

Comparison of New Experimental and Astrophysical F-values For Some Ru-ii Lines, Observed In Hst Spectra of Chi-lupi

Johansson, S. G; Joueizadeh, A; Litzén, Ulf; Larsson, Jörgen; Persson, Anders; Wahlström, Claes-Göran; Svanberg, Sune; Leckrone, D. S; Wahlgren, G. M

[Link to publication]

COMPARISON OF NEW EXPERIMENTAL AND ASTROPHYSICAL f-VALUES FOR SOME Ru II LINES, OBSERVED IN HST SPECTRA OF χ LUPI

SVENERIC G. JOHANSSON,[1,2] ALI JOUEIZADEH[1], ULF LITZÉN,[1] JÖRGEN LARSSON,[3] ANDERS PERSSON,[3]
CLAES-GÖRAN WAHLSTRÖM,[3] SUNE SVANBERG,[3] DAVID S. LECKRONE,[4] AND GLENN M. WAHLGREN[5]

ABSTRACT

We report on experimental absolute oscillator strengths for 18 UV lines of Ru II, obtained by combining laser-induced fluorescence measurements of radiative lifetimes and branching fractions from line intensities in a calibrated Fourier-transform spectrum. HST/GHRS observations of the spectrum of the sharp-lined B star χ Lupi contain six of these lines, for which "astrophysical" relative f-values have been determined. The agreement is within 0.10 dex for a Ru abundance of log $N(Ru)/N(H) = -7.90$, which is 2.3 dex above the solar abundance.

Subject headings: atomic data — line: identification — stars: abundances — stars: individual (χ Lupi) — techniques: spectroscopic — ultraviolet: stars

1. INTRODUCTION

Selected intervals of the ultraviolet spectrum of the chemically peculiar B star χ Lupi have been recorded in highest resolution with the Goddard High Resolution Spectrograph (GHRS) on board the Hubble Space Telescope (HST). In one of the intervals, 1937–1947 Å, obtained with the echelle grating at a spectral resolution of 87,000, three unidentified lines were found to nearly coincide in wavelength with Ru II lines (Leckrone et al. 1991a). However, there was a systematic shift of about 16 mÅ between the laboratory and stellar wavelengths, the latter being accurate to 1–2 mÅ. In order to firmly establish the Ru II identification and to determine the ruthenium abundance in χ Lupi, accurate wavelengths and oscillator strengths for the Ru II lines were needed. Calculated f-values of the lines implied an overabundance of ruthenium in χ Lupi by about a factor of 200 compared to the Sun.

Ruthenium and iron are homologous elements, and the atomic structure of Ru II is therefore similar to Fe II. The ground configuration in Ru II belongs to the complex $(4d + 5s)^7$, and the ground term is $4d^7\ ^4F$ (a^4F in Moore's 1962 notation). The lowest excited subconfiguration of odd parity in Ru II is $4d^6(^5D)5p$, which decays in strong UV multiplets (Moore 1962) to a^4F (UV 1–6), and to a^6D (UV 40–46) and a^4D (UV 75–77) of $4d^6(^5D)5s$. The three lines observed in the 1937–1947 Å interval of χ Lupi belong to UV 4 and UV 5. Recent HST observations of χ Lupi in other wavelength intervals also contain Ru II lines that belong to these low-excitation UV multiplets.

In this paper we report the first experimental f-values for Ru II. We have measured 18 lines from four excited energy levels, and we compare our results with relative "astrophysical" f-values for six of these lines. The experimental

oscillator strengths have been obtained by combining measurements of branching fractions and radiative lifetimes. The branching fractions have been derived from calibrated intensities of Ru II lines recorded with a Fourier-transform (FT) spectrometer. The lifetimes have been measured by means of time-resolved laser-induced fluorescence spectroscopy. Relative "astrophysical" f-values are derived from HST observations by fitting calculated line profiles to the observed lines in the χ Lupi spectrum. The fitting has been performed for each individual line by keeping a preliminary value of the ruthenium abundance constant and adjusting the f-value for the corresponding Ru II transition.

2. WAVELENGTHS

The ruthenium spectrum was emitted from a hollow-cathode discharge. Ruthenium metal cannot be obtained in pieces sufficiently large for making a pure ruthenium hollow cathode. For this reason the cathode was made from a 50 mm long nickel tube with 8 mm inner diameter, and ruthenium powder was placed inside the tube. Neon at 1 torr or argon at 0.2 torr was used as a carrier gas. The strongest Ru II spectrum was obtained from the Ne discharge, while the Ar recordings were used for the intensity calibration (see below).

The spectrum was recorded with a Fourier transform spectrometer. The instrument, manufactured by Chelsea Instruments Ltd., UK, was built according to the principles developed at Imperial College, London (Thorne et al. 1987). It is especially designed to be used at short wavelengths, the lower limit being set at 1750 Å by the transmittance of the quartz optics. After a Fourier transform of the recorded interferogram, the spectrum is obtained on a linear wavenumber scale, which is based on the wavelength of a stabilized He-Ne laser. The scale was calibrated by means of FTS wavelengths (Litzén Brault, & Thorne 1993) of some Ni I lines, which were emitted from the cathode tube in our light source.

Accurate laboratory wavelengths of the Ru II lines that are involved in the branching fraction measurements are presented in Table 1. The wavelengths are derived from the measured wavenumbers and are given in air above 2000 Å and in vacuum below 2000 Å. A conservative estimate of the wavenumber uncertainty is 0.005 cm⁻¹, which corresponds to 0.2 mÅ at 1900 Å and 0.4 mÅ at 3000 Å. The lines at 1939.04 Å and

[1] Department of Physics, University of Lund, Sölvegatan 14, S-223 62 Lund, Sweden.
[2] Lund Observatory, University of Lund, Lund, Sweden.
[3] Division of Atomic Physics, Lund Institute of Technology, P.O. Box 118, S-22100 Lund, Sweden.
[4] Laboratory for Solar Physics and Astronomy, Code 681, NASA/Goddard Space Flight Center, Greenbelt, MD 20771.
[5] Computer Sciences Corporation, Code 681, NASA/Goddard Space Flight Center, Greenbelt, MD 20771.

1939.51 Å appear to be essentially unaffected by blends in the GHRS spectrum of χ Lupi, and for these two lines the agreement between the stellar wavelengths and the new laboratory wavelengths is within the error limits of the stellar observation, viz., ± 2 mÅ (Leckrone et al. 1993a).

3. BRANCHING FRACTIONS

The upper levels of the Ru II lines involved in this work belong to the $4d^6(^5D)5p$ subconfiguration, situated around 6.6 eV above the ground state. These levels have numerous decay channels to levels of the $4d^7$ and $4d^65s$ configurations with transition wavelengths ranging from vacuum-ultraviolet (VUV) to the infrared. In order to derive the oscillator strength for a certain line from the measured lifetime of the upper level, one has to determine the branching fraction, i.e., the fraction of the total radiative decay from the level appearing in that line. In the general case this could be a formidable problem, involving measurements of the intensity of a large number of lines over a wide wavelength range. The spectral response of the spectrometer system must be known over the whole region. In most cases the decay is, however, mainly concentrated to a few strong lines, while the transition rate for all the rest of the decay channels is orders of magnitude lower.

A theoretical calculation (discussed below) shows that more than 85% of the radiative decay of the four energy levels in our study occurs in four to six transitions from each level. All corresponding lines appear in the wavelength range that is accessible to the FTS instrument. Two separate recordings of the spectrum were made in two different regions, due to limited spectral response of the detectors. The detector in the short-wavelength region was a solar blind photomultiplier tube (PMT) with the high-wavelength cutoff at 3000 Å. In order to get a satisfactory signal-to-noise ratio for the lines above 2900 Å, recordings were also made with a second PMT, having the short-wavelength limit at 2500 Å. A number of lines were recorded in the overlap region, and the intensity measurements could thus be put on a common intensity scale.

The intensities of the lines were determined by means of the computer code DECOMP (Brault & Abrams 1989), which permits a Voigt function to be fitted to an observed line. In the present case the parameters of the Voigt function were found to vary among the weaker lines, and for the sake of consistency, we fitted pure Gaussian profiles to all of the lines. The area of the fitted profile was used as the observed intensity of the line.

The major problem with intensity measurements is the calibration of the equipment, i.e., the determination of the efficiency as a function of the wavenumber (or wavelength). Different methods were tried in the present work. A deuterium discharge is known to emit a continuous spectrum over the whole wavelength range studied in the present work, and measurements of its irradiance have been published (Saunders, Ott, & Bridges 1978). Individually calibrated deuterium lamps are also available, and such a lamp was kindly put at our disposal for a test by the Institut für Plasmaphysik, Universität Hannover. This lamp was used for a study of the efficiency of the FTS instrument in the region below 3000 Å. The resulting efficiency curve shows a steep long-wavelength cutoff at the upper limit of the solar blind PMT. The slower decrease at short wavelengths is due to absorption in the silica beamsplitter and a number of quartz windows and lenses. The efficiency curve has a peak at 2500 Å.

A disadvantage with this kind of external intensity calibration is that the front window of the hollow-cathode lamp

emitting the line spectrum is always to some extent contaminated through sputtering during a run. The resulting loss of transmission is most probably wavelength dependent. Moreover, differences in the geometrical distribution of the light from the two light sources may give wavelength dependent differences in the fringe modulation of the recorded interferogram (Thorne 1993). For this reason, intensity calibration by means of internal standards, emitted simultaneously from the same source as the spectral lines being investigated, is highly desirable.

Emission lines that can be used as internal relative intensity standards are available. Adams & Wahling (1981), Danzman & Kock (1982), and Hashiguchi & Hasikuni (1984) have made very careful measurements of the branching fractions of a large number of Ar II lines covering the region from the near-infrared to 2000 Å. The measurements comprise relative intensities of sets of two to 10 lines from common upper levels. The 1 m FTS instrument at the National Solar Observatory, Kitt Peak, was used for the Adams-Whaling and Danzmann-Kock measurements, while a scanning grating instrument was used by Hashiguchi and Hasukini. Different calibration sources were used in different regions. With a few exceptions, the three sets of measurements agree in the region of overlap within the error limits quoted by the authors.

In the present work Ar II lines were used for the efficiency calibration. The Ar-Ru recordings were made immediately before or after the Ne-Ru recordings, which had to be used for observing the weakest of the Ru II lines. Above 3000 Å a consistent efficiency curve could be derived by means of several overlapping sets of Ar II lines. Below 2900 Å, the situation is more difficult as only Ar II lines from the work by Hashiguchi & Hasikuni (1984) are available. In some cases line groups from different upper levels give inconsistent results. It is also difficult to get a reliable connection between the regions above and below 2500 Å. Moreover, no measured branching ratios in Ar II have been reported below 2000 Å.

To overcome some of these difficulties, attempts were made to use published branching ratios of Ge I lines (Lotrian et al. 1978), by introducing small pieces of Ge in the cathode, and CO^+ lines (Ajello 1971), by mixing CO_2 into the carrier gas. In both cases the resulting efficiency curves were internally inconsistent and also incompatible with the general trend of the results obtained from the Ar and deuterium measurements.

The finally adopted efficiency curve for the recording in the region below 3000 Å is obtained from the Ar II lines, see Figure 1. The curve from the deuterium measurements has been used for guiding the choice of Ar lines in cases of inconsistencies and for connecting the regions above and below 2500 Å. The shape of the deuterium curve was also used for extrapolation below 2000 Å.

The resulting branching fractions derived from the observed intensities are presented in Table 1. The table also contains an estimate of the residual branching fractions that are due to all weak lines not observed in the laboratory spectrum. One of these weak lines appears at 1943.966 Å, and it is observed in the stellar spectrum. It has therefore been included in Table 1 represented by its theoretical branching fraction. This theoretical branching fraction as well as the residual ones were obtained from the transition probabilities calculated by means of the Cowan computer code (1981). Two calculations were performed: an ab initio calculation with Hartree-Fock wave functions and a calculation with Slater parameters fitted to observed levels. Both of them comprised the even configurations $4d^7$, $4d^65s$, and $4d^55s^2$ and the odd configuration
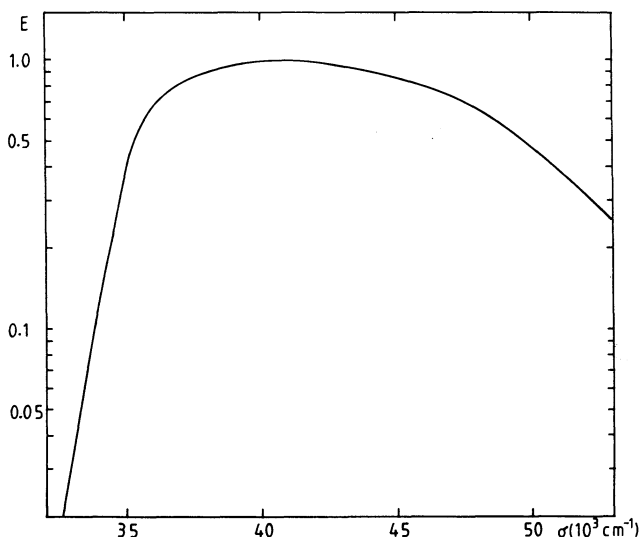
FIG. 1.—Efficency curve for the Fourier-transform spectrometer derived from branching ratios in Ar II emitted by a hollow-cathode lamp.

$4d^6 5p$. The difference between the two calculations as concerns the branching fractions of all the weak transitions was insignificant.

4. RADIATIVE LIFETIMES

In order to obtain radiative lifetimes for the upper levels of the Ru II transitions under study, optical transients following short laser-pulse excitation were recorded. Free ruthenium ions were created in a laser-produced plasma and photoexcited in the expanding plasma by pulsed laser radiation at about 1940 Å.

Ruthenium evaporates at 2300 K, and it is difficult to produce a thermal beam from an oven. Ruthenium ions were therefore produced by irradiating a ruthenium powder with a Q-switched Nd:YAG laser (Lacy et al. 1986, 1989; Bergström et al. 1988); see Figure 2. The powder was confined in a metallic container, which was equipped with 12 mm diameter quartz windows. A pulse energy of 10–50 mJ caused ablation of the ruthenium powder, which was splashing considerably at the laser pulse impact. To maintain a smooth target surface for the laser-pulse excitation, the powder container was positioned on a loudspeaker in a vacuum system. By applying the resonance frequency for the loudspeaker (with container), the powder was shaken to restore the target after each laser pulse. The ablation crater created by the focused laser beam was thus smoothed out before the next pulse arrived 100 ms later.

A Quanta-Ray PDL-1 dye laser, pumped by a Nd:YAG laser, was used to obtain the photo excitation of Ru II by resonance radiation at about 1940 Å. Figure 3 shows the rather special scheme of frequency mixing that had to be applied to produce this radiation. The fundamental radiation of the Nd:YAG laser at 1.064 μm was frequency doubled in a KD*P crystal, and the outcoming beam was doubled in another crystal of the same material. This resulted in a second (0.532 μm) and a fourth (0.266 μm) harmonic, which were separated by a dichroic beamsplitter. The second harmonic at 0.532 μm was used to pump the dye laser, which operated on a LDS 698 dye at approximately 0.715 μm. By mixing this radiation from the dye laser with the fourth harmonic of the Nd:YAG laser at 0.266 μm in a BBO crystal, the required wavelength at 1940 Å

TABLE 1

ATOMIC DATA FOR Ru II TRANSITIONS FROM FOUR ENERGY LEVELS OF THE
ODD-PARITY $4d^6(^5D)5p$ SUBCONFIGURATION

UPPER LEVEL	LOWER LEVEL[a]	MULTIPLET	WAVELENGTH[b] (Å)	WAVENUMBER (cm⁻¹)	B.F.[c]	gf (lab)	log gf (lab)	log gf (star)
$z^4D^o_{5/2}$	$d^7\ ^4F_{7/2}$	UV 5	1903.2209	52542.508	27%	0.33	−0.49	
	$d^7\ ^4F_{5/2}$	UV 5	1939.0434	51571.822	13	0.17	−0.78	−0.76
	$d^7\ ^4P_{3/2}$	UV 30	2192.8634	45588.226	6.0	0.10	−1.01	
	$5s\ ^6D_{5/2}$	UV 44	2313.3562	43213.950	2.3	0.041	−1.39	
	$5s\ ^4D_{7/2}$	UV 76	2882.1095	34686.632	17	0.48	−0.32	
	$5s\ ^4D_{5/2}$	UV 76	2979.7189	33550.420	24	0.70	−0.15	
					Residual: 10			
$z^4D^o_{3/2}$	$d^7\ ^4F_{5/2}$	UV 5	1916.8157	52169.858	30	0.25	−0.60	
	$d^7\ ^4F_{3/2}$	UV 5	1939.5053	51559.539	18	0.15	−0.82	−0.93
	$5s\ ^4D_{5/2}$	UV 76	2927.5341	34148.447	19	0.37	−0.44	
	$5s\ ^4D_{3/2}$	UV 76	2991.6157	33417.005	19	0.38	−0.42	
					Residual: 15			
$z^6P^o_{7/2}$	$d^7\ ^4P_{5/2}$	UV 28	2309.1580	43292.509	1.5	0.027	−1.57	
	$5s\ ^6D_{9/2}$	UV 42	2357.9160	42397.363	30	0.56	−0.25	−0.27
	$5s\ ^6D_{7/2}$	UV 42	2414.8260	41398.267	6.3	0.12	−0.91	
	$5s\ ^6D_{5/2}$	UV 42	2456.4384	40697.026	57	1.15	0.06	
					Residual: 5			
$z^4F^o_{9/2}$	$d^7\ ^4F_{9/2}$	UV 4	1888.0431	52964.893	21	0.29	−0.53	
	$d^7\ ^4F_{7/2}$	UV 4	1943.9505[d]		2.0	0.029	−1.54	−1.54
	$5s\ ^6D_{9/2}$	UV 43	2281.7204	43813.053	9	0.18	−0.74	−0.7
	$5s\ ^6D_{7/2}$	UV 43	2334.9698	42813.975	22	0.47	−0.33	−0.1
	$5s\ ^4D_{7/2}$	UV 75	2976.5837	33585.758	42	1.43	0.16	
					Residual: 3			

[a] Configuration labels: $d^7 = 4d^7$, $5s = 4d^6(^5D)5s$.

[b] Wavelengths in vacuum below 2000 Å, in air above 2000 Å.

[c] Branching fraction. "Residual" gives the sum of all weak lines (see text).

[d] This line is not observed in the laboratory spectrum but in the stellar spectrum. The wavelength is derived from the energy level values with the same accuracy as the measured wavelengths. The branching fraction is a theoretical value (see text).
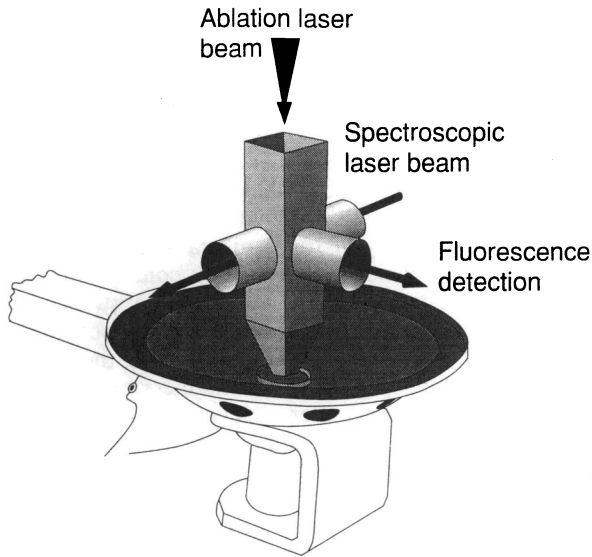
FIG. 2.—Arrangement for production of a ruthenium plasma and observation of laser-induced fluorescence in ruthenium ions.

FIG. 4.—Time-resolved recordings of (a) laser-induced fluorescence from the $z\,^6P_{7/2}$ level of Ru II, and (b) exciting laser pulse.

was obtained. A digital delay generator was utilized as an external trigger for both lasers, allowing the time delay between the plasma-producing pulse and the photoexcitation pulse to be varied. This delay was in the range of 2–6 μs to allow the plasma to partly recombine before the photoexcitation pulse was applied. Since the lifetimes of the excited Ru II levels are short (2–3 ns) there are no problems that the ions "fly out of view" even if the expansion velocity of the plasma is of the order of 10 km s^{-1}. No systematic effects on the measured lifetimes were observed when the time delay and the power of the plasma-producing pulse were varied. By means of a 0.25 m monochromator, the laser-induced fluorescence light was separated from the background plasma radiation. The fluorescence light and the laser pulse were recorded by a microchannel-plate PMT connected to a digital oscilloscope.

To obtain accurate atomic lifetimes from the measured optical transients, it is important that the lifetimes are not too short compared to the length of the photoexciting laser pulse. The Nd:YAG laser pulse is about 10 ns. However, by optimizing the difference in optical path length between the dye laser radiation and the 0.266 μm from the Nd:YAG laser, a resulting pulse length of about 3 ns can be obtained. The temporal structure of the laser system was recorded by turning off the plasma-producing laser and misaligning the 1940 Å beam
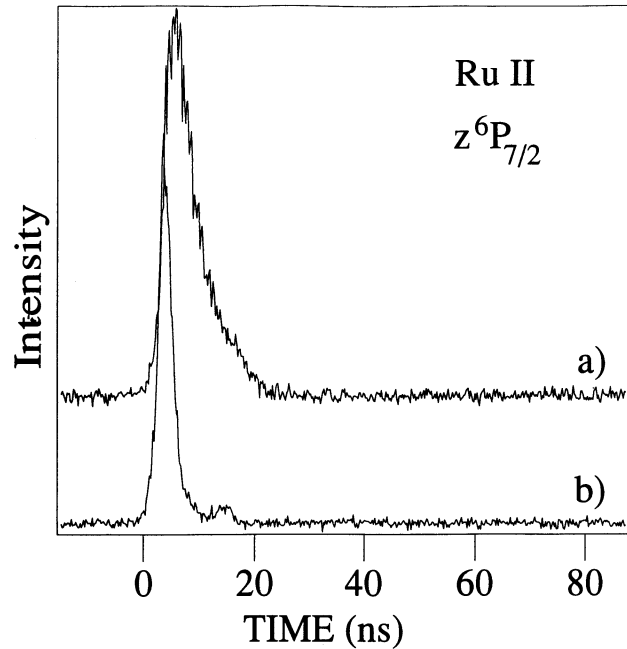
to induce stray light. The temporal structure of the stray light yielded the response function of the system. To accurately extract the short lifetimes of the Ru II states the data were evaluated by fitting a convolution of the system response function and an exponential to the recorded intensity of the fluorescence light. The free parameters in the fitting procedure were intensity, decay constant, pulse position, and background level. To minimize the effects of changes in the excitation pulse, this was recorded for each fluorescence curve. Typical recordings of the photoexcitation laser pulse and the corresponding deexcitation fluorescence signal are shown in Figure 4 for the $z\,^6P_{7/2}$ level. The radiative lifetimes for the four Ru II levels are given in Table 2.

5. EXPERIMENTAL OSCILLATOR STRENGTHS

The branching ratios in Table 1 and the lifetimes in Table 2 were used to derive the experimental oscillator strengths (gf-values) that are given in the seventh column of Table 1. We also give the log gf-values (in the final columns) for comparison with the relative log gf-values derived from the HST spectra (see § 6). The uncertainties of the experimental f-values have to be derived from the uncertainties of the branching fractions and the lifetimes. The latter are rather straightforward to obtain from the fit of the decay curves to the observations, and they are included in Table 2. The uncertainties of the branch-
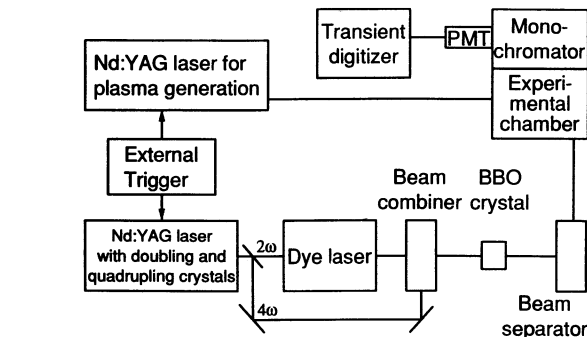

FIG. 3.—Arrangement for generation of the "ablation laser beam" and the "spectroscopic laser beam" (see Fig. 2) from two different Nd:YAG-based laser system.

TABLE 2

LIFETIME DATA FOR FOUR ENERGY LEVELS OF THE $4d^6(^5D)5p$ CONFIGURATION OF Ru II

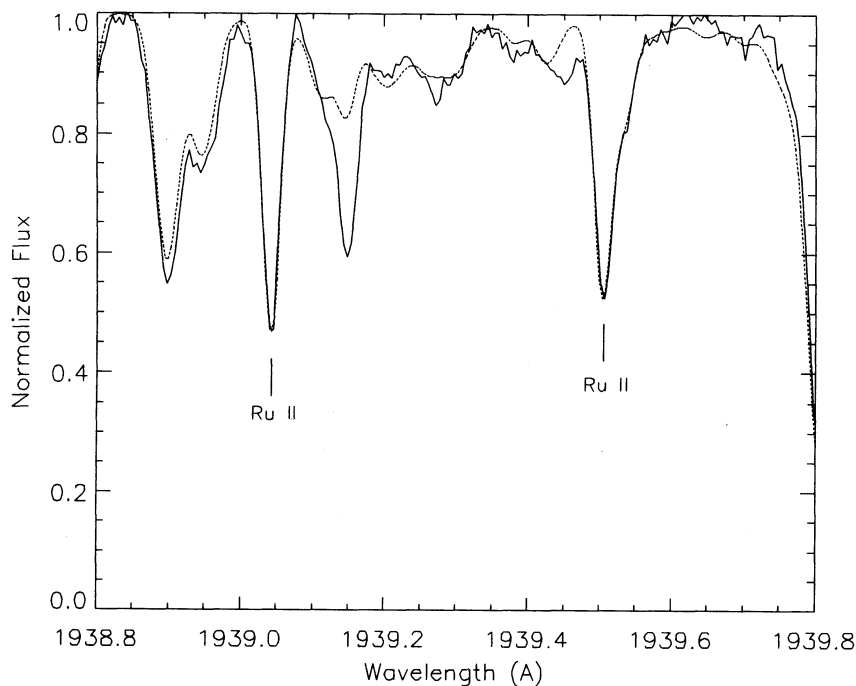| Configuration	Level	Lifetime (ns)	Excitation Wavelength (Å)
$4d^6(^5D)5p$	$z\,^4D^o_{5/2}$	2.7 (3)	1939
	$z\,^4D^o_{3/2}$	2.6 (3)	1939
	$z\,^4F^o_{9/2}$	3.9 (3)	1944
	$z\,^6D^o_{7/2}$	3.6 (3)	1940

FIG. 5.—The GHRS spectrum of χ Lupi around two Ru II lines at 1939 Å. The solid curve is the observation, and the dotted curve, a calculated spectrum

ing fractions are more difficult to estimate, as they depend on the choice of Ar II calibration lines and the weight given to different lines in cases of inconsistency. An estimate has been made by comparing the branching fractions derived from calibration curves that were obtained by means of different sets of Ar II lines and with varying influence from the deuterium calibration. A further source of error in the branching fractions is

the residual intensity in the transitions that were not observed. Considering these uncertainties we estimate the accuracy of the experimental f-values to be better than 25%, which corresponds to 0.10 in the log gf-value.

A serious source of error that may affect emission measurements is self-absorption. It is likely to appear in many of the lines observed in this work, as they are transitions to the
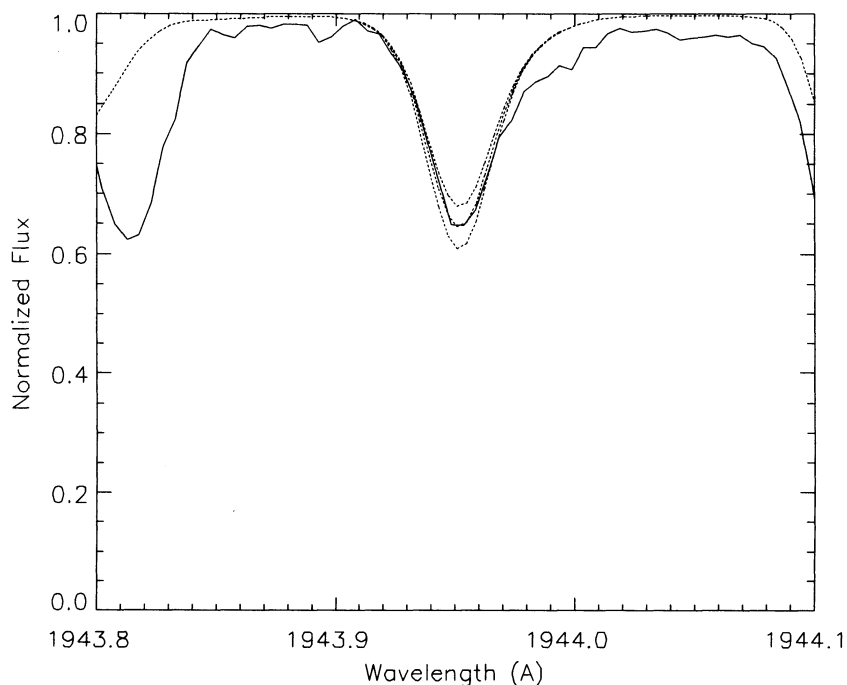

FIG. 6.—A Ru II line at 1943.95 Å in the GHRS spectrum (*solid curve*) of χ Lupi illustrating the sensitivity in deriving "astrophysical f-values." The dashed curves show the calculated spectrum at three different log gf-values for the Ru II line (*from top*): −1.64, −1.54, and −1.44, where −1.54 gives the best fit.

ground term or to other very low levels. The self-absorption is, however, believed to be negligible as the density of ruthenium sputtered from powder inside the nickel cathode is small. No distortion of the line profiles by self-absorption was observed.

6. "ASTROPHYSICAL" RELATIVE f-VALUES FROM HST/GHRS SPECTRA

In 1991 January, the spectrum of the chemically peculiar B star χ Lupi was recorded in highest resolution with the Goddard High Resolution Spectrograph (GHRS) (Leckrone et al. 1991a). Three lines were tentatively identified as Ru II in a single 10 Å echelle observation that was centered on the resonance line of Hg II at 1942 Å (Leckrone, Wahlgren, & Johansson, 1991b). Revised wavelengths from our new FTS measurements confirmed the identifications. On the basis of preliminary calculations of transition probabilities in Ru II and for experimental f-values for the corresponding transitions in the homologous spectrum Fe II (Kroll & Kock 1987), the ruthenium abundance in χ Lupi was determined by means of these three lines to be log $N(Ru)/N(H) = -7.90$ (Leckrone et al. 1993b). This is 2.26 dex above the solar value. Two of the three Ru II lines are shown in Figure 5. Later HST observations of χ Lupi in other wavelength intervals show more Ru II lines, all of them from energy levels with a low excitation energy.

By adopting the preliminary value of the ruthenium abundance of −7.90 we have determined relative "astrophysical" f-values for six of the Ru II lines in Table 1. One more transition from the $^4F_{9/2}$ level at 1943.966 Å is observed in the stellar spectrum but not in the laboratory spectrum. However, for this line we have used the theoretical branching fraction from the calculations and converted to a log gf-value, which has been inserted in Table 1 and compared with the astrophysical log gf-value.

The "astrophysical" f-value, or log gf-value, for each of the observed Ru II lines has been obtained by adjusting this parameter in a synthetic spectrum until the calculated line profile agrees with the observed line profile. The procedure is illustrated in Figure 6, where we compare the observed line profile of the Ru II line at 1943 Å with calculated line profiles at three different log gf-values: The best value, and the best value ±0.10 dex. The uncertainty for well-defined lines is estimated to be about 0.05 dex, i.e., 0.05 on the logarithmic scale, which corresponds to about 12%.

The GHRS spectrum of χ Lupi around the three Ru II lines above 2000 Å are shown in Figure 7 together with synthetic spectra. The log gf-values used for the Ru II lines to fit the calculated spectrum to the observations should be considered as upper limits. The 2281.72 Å feature is reproduced quite well with a log gf-value of −0.7, leaving some missing opacity in the wings. The experimental value is −0.74. The stellar line at 2334.97 Å is probably blended by an unknown line in the core and another line in the blue wing. This is supported by the discrepancy between the experimental and astrophysical f-values for this line. A larger f-value for the third line at 2357.92 Å makes the overall fit worse, which might imply a contribution from another line. This could be due to an Ag II transition at 2357.917 Å (Kalus 1993). The line at 2357.95 Å belongs to Fe II.

The agreement between the experimental absolute log gf-values and the "astrophysical" relative log gf-values is in general very good and within the combined uncertainties. Since there is no systematic shift between the experimental and
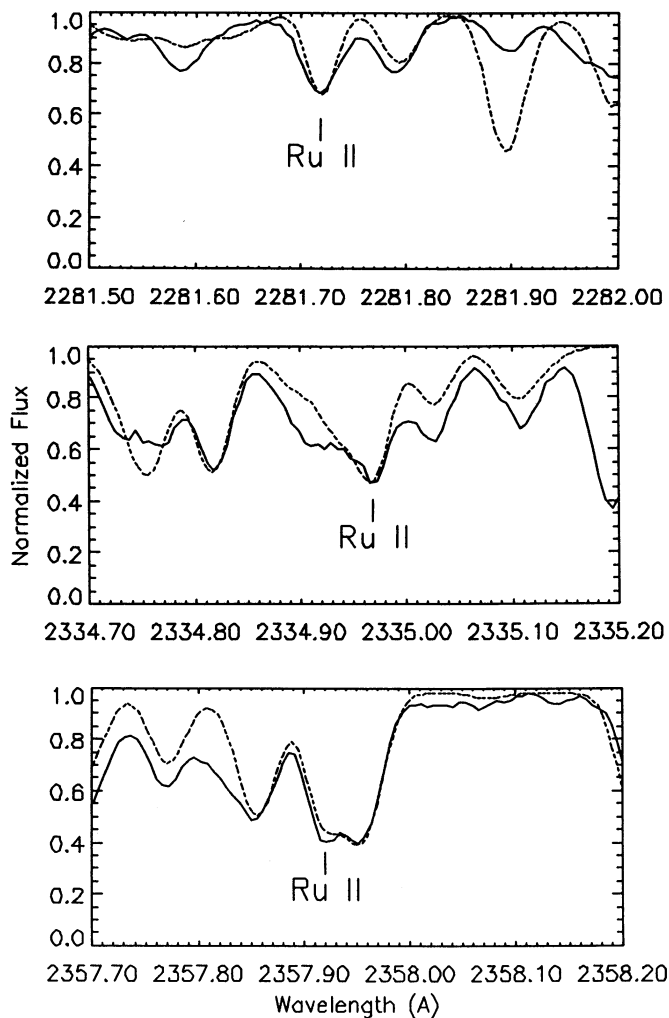

FIG. 7.—Pieces (0.5 Å) of the GHRS spectrum (solid curve) of χ Lupi showing three Ru II lines above 2000 Å. The dashed curves represent calculated spectra with upper limits of the log gf-values for the Ru II lines.

"astrophysical" oscillator strengths, the ruthenium abundance in χ Lupi of log $N(Ru)/N(H) = -7.90$ is accurate to 25%.

7. CONCLUSIONS

The present study confirms the identification of Ru II lines in the UV spectrum of χ Lupi, with a high degree of confidence, and verifies the 2.3 dex overabundance of ruthenium relative to the Sun. We believe this is the first robust detection of Ru II lines in a stellar spectrum; it is certainly the first ruthenium abundance derived for an early-type star. This is an important component of the campaign described by Leckrone et al. (1993b) to "fill in" the periodic table with accurate elemental abundances in order to tightly constrain models for the origin of anomalous abundance patterns in chemically peculiar stars like χ Lupi.

We have compared experimental oscillator strengths of Ru II, obtained by branching fraction measurements in emission and ionic lifetime measurements, with relative oscillator strengths derived from absorption lines in the UV spectrum of χ Lupi. The consistent results imply that high-resolution stellar spectra can provide a valuable test of the experimental method

used to get absolute oscillator strengths. By combining different advanced techniques, it is possible to obtain experimental atomic data that match the accuracy of high signal-to-noise ratio observations of sharp-lined stars with the Goddard High Resolution Spectrograph on board the *Hubble Space Telescope*. The previous limits on lifetime measurements set by the laser pulse length and the accessible wavelength regions are constantly being widened due to the advent of new laser systems. Highly accurate wavelengths can be obtained from FTS instruments all over the region from the infrared down to 1750 Å. At shorter wavelengths, sufficient accuracy can be obtained with high dispersion grating spectrographs. The main uncertainty comes from the branching ratio measurements due to the lack of internal calibration lines in the short wavelength region.

REFERENCES

Adams, D. L., & Whaling, W. 1981, J. Opt. Soc. Am., 71, 1036
Ajello, J. M. 1971, J. Chem. Phys., 55, 3158
Bergström, H., Faris, G. W., Hallstadius, H., Lundberg, H., Persson, A., & Wahlström, C.-G. 1988, Z. Phys., D8, 17
Brault, J. W., & Abrams, M. C. 1989, High Resolution Fourier Transform Spectroscopy, OSA Technical Digest Series, vol. 6 (Washington: Optical Society of America), 110
Cowan, R. D. 1981, The Theory of Atomic Structure and Spectra (Berkeley: Univ. of California Press)
Danzmann, K., & Kock, M. 1982, J. Opt. Soc. Am., 72, 1556
Hashigushi, S. & Hasukini, M., 1985, J. Phys. Soc. Japan, 54, 1290
Kalus, G. 1993, Diploma work, Department of Physics, Univ. of Lund
Kroll, S., & Kock, M. 1987, A&AS, 67, 225
Lacy, R. A., Nilsson, A. C., Byer, R. L., Silvfast, W. T., Wood, O. R., II, & Svanberg, S. 1986, in Short Wavelength Coherent Radiation: Generation and Applications, ed. D. T. Attwood & J. Bokor (AIP Conf. Proc. 147) (New York: AIP)
———. 1989, J. Opt. Soc. Am., B6, 1209

Leckrone, D. S., Johansson, S. G., & Wahlgren, G. M. 1991a, in *HST* Workshop: The Year of First Light, ed. A. L. Kinney & J. C. Blades (Baltimore: Space Telescope Science Institute), 83
Leckrone, D. S., Johansson, S., Wahlgren, G. M., & Adelman, S. J. 1993a, Phys. Scripta, T47, 149
Leckrone, D. S., Wahlgren, G. M., & Johansson, S. G. 1991b, ApJ, 377, L37
Leckrone, D. S., Wahlgren, G. M., Johansson, S. G., & Adelman, S. J. 1993b, IAU Colloq. 138, Peculiar versus Normal Phenomena in A-Type and in Related Stars, ed. M. M. Dworetsky, F. Castelli, & R. Faraggiana (ASP Conf. Proc. 44), 42
Litzén, U., Brault, J. W., & Thorne, A. P. 1993, Phys. Scipta, 47, 628
Lotrian, J., Cariou, J., Guern, Y., & Johannin-Gilles, A. 1978, J. Phys. B, 11, 2273
Moore, C. E. 1962, An Ultraviolet Multiplet Table (NBS. Circ. 488), § 3
Saunders, R. D., Ott, W. R., & Bridges, J. M. 1978, Appl. Opt., 4, 593
Thorne, A. P. 1993, private communication
Thorne, A. P., Harris, C. J., Wynne-Jones, I., Learner, R. C. M., & Cox, G. 1987, J. Phys. E, 20, 54